

10th CIRP Conference on Photonic Technologies [LANE 2018]

# Optimization of process parameters in laser transmission welding for food packaging applications

J. Griffiths<sup>a,\*</sup>, C. Dowding<sup>a</sup>

<sup>a</sup>*School of Engineering, University of Lincoln, Brayford Pool, Lincoln, LN6 7TS, United Kingdom*

\* Corresponding author. Tel.: +441522837936. E-mail address: [jgriffiths@lincoln.ac.uk](mailto:jgriffiths@lincoln.ac.uk)

## Abstract

Plastics' joining is used widely in food processing applications for the packaging of increasingly diverse food products. Laser transmission welding is an attractive proposition for such applications as it can significantly reduce tooling costs and potential downtime at product changeovers. In order to fulfil this promise in an industrial environment, an effective means of process parameter prediction is required. In this paper, goal driven optimization is conducted, utilizing numerical simulations as the basis for the prediction of optimal process parameters for the laser transmission welding of polyethylene film to a polypropylene substrate. A key consideration of the optimization process is the requirement for specific, pre-defined bonded track widths.

© 2018 The Authors. Published by Elsevier Ltd. This is an open access article under the CC BY-NC-ND license

(<https://creativecommons.org/licenses/by-nc-nd/4.0/>)

Peer-review under responsibility of the Bayerisches Laserzentrum GmbH.

*Keywords:* Laser; Finite Element; Optimization; Response Surface; MOGA.

## 1. Introduction

Laser transmission welding of polymers is a versatile method of plastics joining with a wide range of applications. The process involves the transmission of laser radiation, typically visible to infrared, through an optically transparent film and subsequent absorption of the laser radiation at an interface with an opaque substrate. The resulting temperature rise at this interface is used to either activate a resin or cause melting to form a weld between the two materials [1].

The main advantage of laser transmission welding over conventional plastics joining techniques is its inherent flexibility, a result of the non-contact nature of the process. A particularly promising application area for laser transmission welding is food packaging, specifically the joining of a clear film to an opaque substrate in the packaging of ready meals [2]. A key barrier to the application of laser transmission welding in food packaging applications has been the requirement for an effective means of process parameter prediction.

The work presented in this paper outlines a method for process parameter prediction based on goal driven optimization of numerical simulations of the laser heating process. A key constraint for the optimization process is the requirement for specific, pre-defined bonded track widths.

## 2. Methodology

### 2.1. Experimental set-up

For this work, a bespoke material handling rig was developed in order to bring a 600 mm wide, 75 µm thick polyethylene film into contact with a 0.64 mm thick opaque isotactic polypropylene substrate for the purposes of laser transmission welding [3]. The polyethylene film was supplied pre-coated with a thin layer of thermally activated adhesive. The rig comprised a CO<sub>2</sub> laser source (Fenix Flyer, Synrad, Inc.) with integrated scanning galvanometer. The working distance of the laser at focus was 450 mm. The film was drawn taut over the substrate using clutched reels. The substrate could subsequently be brought into contact with the

film by raising its height using a variable height stage. The incident laser spot diameter could be altered by varying working distance. This was achieved by varying the height of the laser source. The experimental set-up is shown in Figure 1.

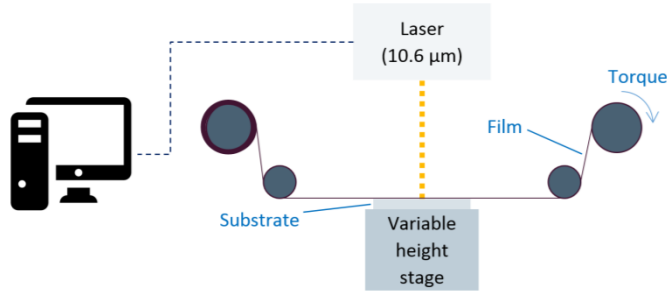


Fig. 1. Experimental set-up of the material handling rig.

### 2.2. Peel force measurement

The strength of the bond between the film and the substrate was determined by measuring the peel force using a tensile tester (3340 Single Column Testing System, Instron Corp.) with a bespoke translation peel testing accessory (Constant 90° Angle Peel Fixture, Instron Corp.) according to the standard ASTM: B571. The peel rate and sampling frequency were kept constant at 5 mm/s and 100 Hz, respectively, for all measurements. The peak peel resistance force were extracted from the software (Bluchill 2, Instron Corp.) for further analysis.

### 2.3. Finite element model development

A transient-thermal finite element model of the laser heating of polypropylene was developed in ANSYS Workbench (Version 18.1). The governing equation for conduction in the thermal analysis is:

$$\rho C_p \frac{\delta T}{\delta t} = \nabla \cdot (k \nabla T) \quad (1)$$

where  $\rho$  is the density (kg/m<sup>3</sup>),  $C_p$  is the specific heat capacity (J/kgK),  $T$  is the temperature (K),  $t$  is the time (s) and  $k$  is the thermal conductivity (W/mK). The term  $\nabla$  is the differential or gradient operator (sometimes referred to as the Nabla operator) for three dimensional Cartesian co-ordinate systems. All boundaries were subject to convective and radiative heat transfer. Therefore, the heat flux  $q$  (W/m<sup>2</sup>) at a given boundary is given by:

$$-n \cdot q = q_0 + h(T_{amb} - T) + \varepsilon \sigma (T_{amb}^4 - T^4) \quad (2)$$

where  $n$  is the normal vector of the boundary,  $h$  is the heat transfer co-efficient (W/m<sup>2</sup>K),  $T_{amb}$  is the ambient temperature (K),  $\varepsilon$  is the surface emissivity (1) and  $\sigma_s$  is the Stefan Boltzmann constant (W/m<sup>2</sup>K<sup>4</sup>) [4].

The intensity distribution  $I$  (W/m<sup>2</sup>) of the incident laser beam was approximated by a Gaussian distributed heat source, modelled using ANSYS Parametric Design Language (APDL). The Gaussian heat source is described by Eq. 3:

$$I = I_0 e^{-\left(\frac{2r^2}{\omega_0^2}\right)} = \frac{2P}{\pi\omega_0^2} e^{-\left(\frac{2r^2}{\omega_0^2}\right)} \quad (3)$$

where  $I_0$  is the peak intensity (W/m<sup>2</sup>),  $P$  is the average laser power (W),  $r$  is radial distance (m) and  $\omega_0$  is the beam radius (m). An absorption co-efficient of 95.87% was specified for all simulations conducted, based on values for the refractive index and extinction coefficient of isotactic polypropylene.

A plane of symmetry was specified along the  $zx$ -axis in order to reduce the problem size and increase the computational efficiency of the simulation. Globally, the mesh element size was set to fine and determined by automatic meshing in ANSYS. A suitable maximum element size for use along the irradiation path was determined by a convergence study and found to be 50 μm. An example output from the model is shown in Figure 2.

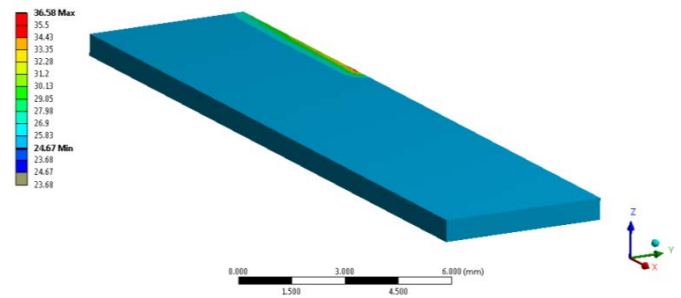


Fig. 2. Typical temperature output (°C) from the transient-thermal finite element model (5 x 20 x 0.64 mm polypropylene, 0.6 mm spot size, 40 mm/s traverse speed, 8 W laser power, 85% absorption).

## 3. Results and discussion

The experimental work focused on determining the effect of laser power ( $P$ ), traverse speed ( $v_0$ ) and spot size ( $d_0$ ) on measured peel force. The numerical work focused on process parameter prediction by means of a multi-objective, goal driven optimization.

The aim of the work was to predict optimal process parameters for laser transmission welding/bonding of polyethylene film to a polypropylene substrate. The work focused on (i) determination of the influence of process parameters on measured peel force and (ii) prediction of optimal process parameters.

### 3.1. Effect of laser parameters on measured peel force

A custom 672 design point parametric study was conducted in which the variables were  $P$ ,  $v_0$  and  $d_0$ . The upper and lower bounds for the parametric study are given in Table 1.

Table 1. Input process parameters and their ranges for the parametric study.

| Input variable | Lower bound | Upper bound |
|----------------|-------------|-------------|
| P (W)          | 4           | 27          |
| $v_0$ (mm/s)   | 35          | 85          |
| $d_0$ (mm)     | 0.6         | 2           |

At each design point, the beam was traversed over a length of 15 mm with the aim of forming a bond between the film and substrate. Subsequently, the peel force was measured. At total of 480 of the 672 design points tested resulted in bonding between the film and substrate.

A useful parameter to consider when analyzing the effect of laser power, traverse speed and spot size on the measured peel force is the irradiant exposure ( $I_r$ ), as defined by Eq. 4, which is dimensionally equivalent to the energy density of the beam:

$$I_r = \frac{Pd_0}{\pi v_0 \omega_0^2} \quad (4)$$

The measured peel force as a function of  $I_r$  is shown in Figure 3.

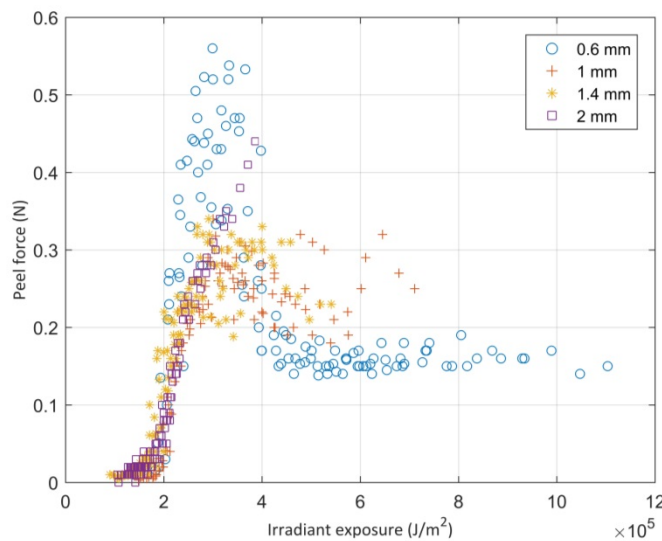


Fig. 3. Measured peel force as a function of irradiant exposure.

Figure 3 reveals three distinct regimes. At irradiant exposures of less than  $2.2 \times 10^5 \text{ J/m}^2$ , a weak bonding regime exists in which bonds with measured peel forces of less than 0.1 N, in the majority of cases, are formed. As the irradiant exposure approaches  $2.2 \times 10^5 \text{ J/m}^2$ , peel forces in excess of 0.1 N are measured but there remains a high degree of variability. For  $I_r$  values of between  $2.2 \times 10^5 \text{ J/m}^2$  and  $2.5 \times 10^5 \text{ J/m}^2$ , a consistent bonding regime is observed, in which measured peel forces lie invariably in the region of 0.1 N to 0.4 N. At  $I_r$  values of above  $2.5 \times 10^5 \text{ J/m}^2$  the variability in measured peel force for a given  $I_r$  increases.

In order to rationalize these experimental observations, the complex interrelation of process parameters was characterized through use of a finite element simulation of the laser heating of polypropylene. A 40 simulation parametric study was conducted, based on a random sampling of the design space using Latin Hypercube sampling, the aim of which was to determine the peak temperature on the top surface of the polypropylene substrate (*i.e.* the bonding interface) as a function of process parameters. The input parameters were  $P$ ,  $v_0$  and  $d_0$ . The search domain is given in Table 1, the bounds of which reflect the full range of parameters used in the experimental study. The results of the parametric numerical

study are shown in Figure 4, revealing a strong positive quadratic correlation between  $I_r$  and peak surface temperature over the specified search domain, with a coefficient of determination ( $R^2$ ) of 93.35%. Simulated temperatures for  $I_r$  values associated with the weak and consistent bonding regimes (that is, up to  $2.5 \times 10^5 \text{ J/m}^2$ ) are below or close to the melting temperature of isotactic polypropylene ( $171 \text{ }^\circ\text{C}$ ) [4]. This suggests that the mechanism of joining in the consistent bond regime involves thermal activation of the adhesive on the polyethylene film as opposed to laser welding by melting. As the irradiant exposure surpasses  $2.5 \times 10^5 \text{ J/m}^2$ , the mechanism is increasingly dominated by melting.

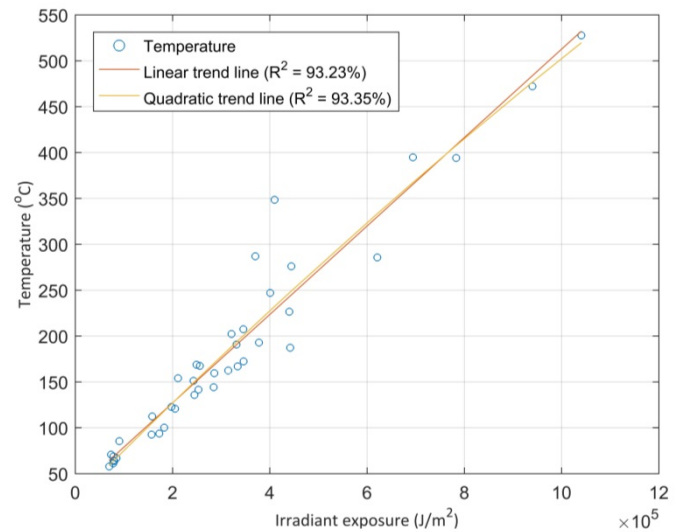


Fig. 4. Maximum predicted temperature as a function of irradiant exposure.

### 3.2. Optimal process parameter prediction

Optimal processes parameters were predicted through application of a response surface optimization using the multi-objective genetic algorithm (MOGA) in ANSYS Workbench. A 29 simulation parametric study was conducted, with design points chosen according to the enhanced rotatable central composite design method of design of experiments. The input parameters were  $P$ ,  $v_0$  and  $d_0$ . The search domain is given in Table 1. A second order polynomial was used to generate the response surface.

The objective of the optimization was to produce peel forces ( $F$ ) in the range of 0.1 N to 0.4 N though specification of thermally activated adhesive bonding as the mechanism of joining. To achieve this, the simultaneous goals and constraints for the MOGA optimization process were specified as follows:

- Seek a target  $d_0$  (higher importance);
- maximize  $I_r$  to within an upper bound of  $2.5 \times 10^5 \text{ J/cm}^2$  (default importance) and;
- maximize the peak surface temperature ( $T$ ) to within an upper bound of  $171^\circ\text{C}$ , the melting temperature of polypropylene (default importance).

The results of the optimization (that is, candidate points A, B and C), their subsequent numerical verification and

validation against the closest corresponding experimental design point are shown in Tables 2-5.

Table 2. Results of the MOGA optimization (target  $d_0 = 0.6$  mm).

|              | $P$<br>(W) | $v_0$<br>(mm/s) | $d_0$<br>(mm) | $T$ (°C) | $I_r$ (J/m <sup>2</sup> ) | $F$<br>(N) |
|--------------|------------|-----------------|---------------|----------|---------------------------|------------|
| Candidate A  | 6.30       | 56.06           | 0.60          | 170.32   | 2.38x10 <sup>5</sup>      | -          |
| Verification |            |                 |               | 174.77   |                           |            |
| Validation   | 5.97       | 54.00           | 0.60          | -        | 2.35x10 <sup>5</sup>      | 0.41       |
| Candidate B  | 7.17       | 59.25           | 0.65          | 170.86   | 2.39x10 <sup>5</sup>      | -          |
| Verification |            |                 |               | 172.42   |                           |            |
| Validation   | 7.38       | 60.75           | 0.60          | -        | 2.58x10 <sup>5</sup>      | 0.44       |
| Candidate C  | 9.21       | 62.76           | 0.76          | 170.37   | 2.45x10 <sup>5</sup>      | -          |
| Verification |            |                 |               | 170.32   |                           |            |
| Validation   | 9.44       | 60.75           | 0.60          | -        | 3.34x10 <sup>5</sup>      | 0.36       |

Table 3. Results of the MOGA optimization (target  $d_0 = 1$  mm).

|              | $P$<br>(W) | $v_0$<br>(mm/s) | $d_0$<br>(mm) | $T$ (°C) | $I_r$ (J/m <sup>2</sup> ) | $F$<br>(N) |
|--------------|------------|-----------------|---------------|----------|---------------------------|------------|
| Candidate A  | 14.54      | 73.49           | 1.02          | 168.88   | 2.47x10 <sup>5</sup>      | -          |
| Verification |            |                 |               | 165.67   |                           |            |
| Validation   | 14.57      | 74.25           | 1.00          | -        | 2.50x10 <sup>5</sup>      | 0.23       |
| Candidate B  | 11.65      | 59.68           | 0.99          | 158.17   | 2.50x10 <sup>5</sup>      | -          |
| Verification |            |                 |               | 157.52   |                           |            |
| Validation   | 11.42      | 60.75           | 1.00          | -        | 2.39x10 <sup>5</sup>      | 0.18       |
| Candidate C  | 17.12      | 82.45           | 1.09          | 169.48   | 2.42x10 <sup>5</sup>      | -          |
| Verification |            |                 |               | 166.74   |                           |            |
| Validation   | 16.95      | 81.00           | 1.00          | -        | 2.66x10 <sup>5</sup>      | 0.23       |

Table 4. Results of the MOGA optimization (target  $d_0 = 1.4$  mm).

|              | $P$<br>(W) | $v_0$<br>(mm/s) | $d_0$<br>(mm) | $T$ (°C) | $I_r$ (J/m <sup>2</sup> ) | $F$<br>(N) |
|--------------|------------|-----------------|---------------|----------|---------------------------|------------|
| Candidate A  | 19.85      | 69.12           | 1.45          | 147.55   | 2.52x10 <sup>5</sup>      | -          |
| Verification |            |                 |               | 149.73   |                           |            |
| Validation   | 19.74      | 67.50           | 1.40          | -        | 2.66x10 <sup>5</sup>      | 0.24       |
| Candidate B  | 17.56      | 72.73           | 1.23          | 157.60   | 2.50x10 <sup>5</sup>      | -          |
| Verification |            |                 |               | 157.22   |                           |            |
| Validation   | 17.52      | 74.25           | 1.40          | -        | 2.15x10 <sup>5</sup>      | 0.21       |
| Candidate C  | 18.58      | 77.48           | 1.23          | 160.66   | 2.49x10 <sup>5</sup>      | -          |
| Verification |            |                 |               | 160.11   |                           |            |
| Validation   | 18.65      | 74.25           | 1.40          | -        | 2.28x10 <sup>5</sup>      | 0.24       |

Table 5. Results of the MOGA optimization (target  $d_0 = 2$  mm).

|              | $P$<br>(W) | $v_0$<br>(mm/s) | $d_0$<br>(mm) | $T$ (°C) | $I_r$ (J/m <sup>2</sup> ) | $F$<br>(N) |
|--------------|------------|-----------------|---------------|----------|---------------------------|------------|
| Candidate A  | 20.02      | 52.52           | 1.99          | 128.18   | 2.44x10 <sup>5</sup>      | -          |
| Verification |            |                 |               | 124.20   |                           |            |
| Validation   | 20.27      | 54.00           | 2.00          | -        | 2.39x10 <sup>5</sup>      | 0.21       |
| Candidate B  | 12.98      | 36.11           | 1.85          | 120.42   | 2.47x10 <sup>5</sup>      | -          |
| Verification |            |                 |               | 117.13   |                           |            |
| Validation   | 12.71      | 40.00           | 2.00          | -        | 2.02x10 <sup>5</sup>      | 0.07       |
| Candidate C  | 18.58      | 77.48           | 1.23          | 160.66   | 2.49x10 <sup>5</sup>      | -          |
| Verification |            |                 |               | 160.11   |                           |            |
| Validation   | 18.09      | 74.25           | 2.00          | -        | 1.55x10 <sup>5</sup>      | 0.02       |

Upon validation against the closest corresponding experimental design point it can be seen that candidates listed in Tables 2, 3 and 4 fall within or close to the consistent bond regime associated with thermally activated adhesive bonding.

However, the algorithm fares less well at a target  $d_0$  of 2 mm. Only one of the three candidate points in Table 5 fall within the consistent bond regime upon validation against the closest corresponding experimental design point. This can be attributed to the sensitivity of maximum temperature to the input parameters, shown in Figure 5. As the spot size increases, the sensitivity of maximum temperature to  $P$  and  $v_0$  is increasingly marginalized by  $d_0$ , which has the largest magnitude of influence.

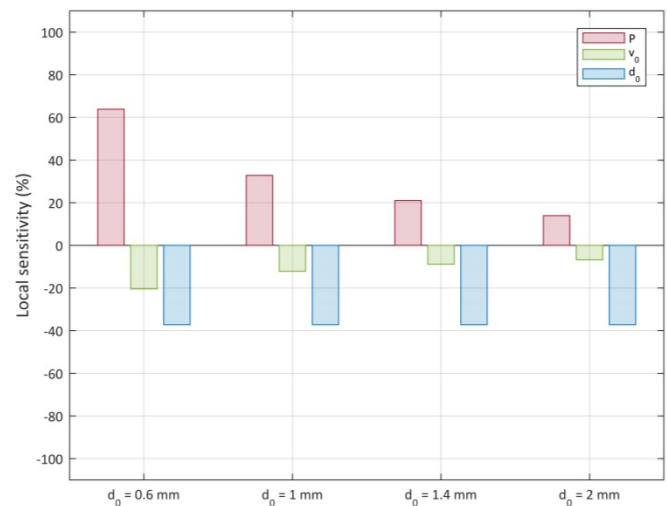


Fig. 5. Local sensitivities of maximum predicted temperature ( $P = 15.73$  W,  $v_0 = 60.5$  mm/s).

#### 4. Conclusions

An experimental and numerical study into the laser transmission welding of polyethylene film to a polypropylene substrate has been conducted. A correlation between the measured peel force and irradiant exposure ( $I_r$ ) was observed experimentally. In conjunction with results from numerical simulations of laser heating, a consistent bond regime producing peel forces of between of 0.1 N to 0.4 N was identified in which thermal activation of the adhesive on the polyethylene film was the mechanism of joining. Optimal process parameter combinations were predicted numerically through application of a multi-objective genetic algorithm. The goal of the optimization was to produce peel forces in consistent bond regime for a specified spot diameter. Validation against the closest corresponding experimental design point showed that this is an effective means of process parameter prediction.

#### References

- [1] Brown N, Kerr D, Parkin RM, Jackson MR, Shi F. Non-contact laser sealing of thin polyester food packaging films. Optics and Lasers in Engineering 2012 10;50(10):1466-1473.
- [2] Pagano N, Campana G, Fiorini M, Morelli R. Laser transmission welding of polylactide to aluminium thin films for applications in the food packaging industry. Optics & Laser Technology 2017 1 June 2017;91:80-84
- [3] Dowding C, Dowding R, Griffiths J, Lawrence J. Peel resistance characterization of localized polymer film bonding via thin film adhesive thermally activated by scanned CO2 laser. Optics & Laser Technology 2013 June 2013;48:358-365.

- [4] Brandrup J, Immergut EH. Polymer Handbook. 3rd ed. USA: John Wiley and Sons.